Nuclear binding energies from moment methods: Realistic effective no-core Hamiltonian

F. J. Margetan
Ames Laboratory, Department of Energy and Department of Physics, Iowa State University, Ames, Iowa 50011

J. P. Vary
Arizona Research Laboratories, University of Arizona
and Department of Physics, Iowa State University, Ames, Iowa 50011
(Received 4 March 1983)

Total binding energies for nuclei with $14 \leq A \leq 18$ are obtained from a realistic effective no-core Hamiltonian, H_{eff}, using moment methods. The lowest few moments of H_{eff} are evaluated in an oscillator model space of four major shells. These moments are then used to determine a number of continuous and discrete density of states functions, each of which yields an estimate for the H_{eff} ground state energy. The adjustable discrete density of states functions which we introduce are based upon realistic single-particle Hamiltonians. With a reasonable selection of moment method ingredients we obtain good agreement between theory and experiment for relative binding energies within each A chain. The most stable isobar is correctly predicted in all cases and Coulomb energy differences are in close agreement with experiment. Thus, the valley of β stability is well reproduced in this approach with a simple overall shift in absolute binding energies for each A chain.

[NUCLEAR STRUCTURE Binding energies from moment methods; spectral properties of realistic effective no-core Hamiltonian; approximate density of states function based on realistic single-particle Hamiltonians.]

I. INTRODUCTION

One of the long standing goals of nuclear theory has been to test the hypothesis that the nuclear ground state and low-lying excitations could be primarily understood within a nonrelativistic framework using an interaction which fits two-nucleon experiments. The most convincing evidence to date that this hypothesis may be *false* comes from the coupled cluster [or exp(s)] calculations of the Bochum group.[1] For example, with a realistic nucleon-nucleon interaction, they find that theory underbinds ^{16}O by 38% and underbinds ^{40}Ca by 30%. On the other hand, the exp(s) results for ^{17}O and ^{18}O (Ref. 2) indicate that somewhat better *relative* binding energies and spectral properties may be obtained. Also, reasonable excited state spectra for ^{16}O are obtained.[3]

The present work employs moment methods (MM's) with the goal to investigate the conclusions of the exp(s) method and to extend the discussion to ground states of a larger range of nuclei in the $A = 16$ region. Our results are consistent with those of the exp(s) method but we employ quite a different set of approximations.

Our earliest effort[4] applied MM's to obtain binding energies of *s-d* shell nuclei with respect to ^{16}O using realistic effective shell model Hamiltonians. Later, we presented preliminary results[5,6] of the present investigation where realistic no-core Hamiltonians were used to obtain the binding energy of ^{16}O. As these applications grew in scope we felt a need to assess the overall accuracy of MM's when only the few lowest moments were used in very large model spaces to predict the ground state (g.s.) energy for a given Hamiltonian. We thus performed an extensive set of tests of the MM approach using a soluble Hamiltonian in ultralarge model spaces.[7] This most recent effort (hereafter referred to as I) serves to guide the realistic calculations on which we report here.

One concern for accuracy arises because the physically interesting low-energy part of the nuclear spectrum lies several standard deviations from the centroid of the density of states (DOS) function, $\rho(E)$, in typical applications with large model spaces. Therefore, in I we assessed the accuracy of extrapolating into this low-energy region from a knowledge of the first few moments of $\rho(E)$ using the soluble harmonic oscillator Hamiltonian. The accuracy was studied as a function of model space size, parametrization chosen for $\rho(E)$, method of truncation of the model space, and other ingredients. The basic conclusions in I were fourfold:

(1) To a good approximation the error in the MM estimate of the g.s. energy grew only linearly with the logarithm of the many-body basis space dimensionality.

(2) The standard truncation scheme based on single particle energies ("energy truncation scheme") led to the lowest absolute errors and to the least dependence on the parametrization chosen for $\rho(E)$.

(3) The two-moment Gaussian DOS distribution and the three-moment Weibull distribution, led to the lowest absolute errors and the least dependence of the error on model space dimensionality.

(4) Errors in relative ground state energies for $14 \leq A \leq 18$ were much smaller and less dimensionality dependent than errors in total energies.

Based upon the conclusions of I we have applied MM's with an optimum choice of ingredients to obtain binding energies of $14 \leq A \leq 18$ nuclei from a realistic no-core Hamiltonian. Our primary concentration is on relative binding energies, especially binding energy differences

within A chains, since MM's are expected to be most accurate there, and since the exp(s) results imply that reasonable agreement between theory and experiment might be obtained.

We proceed in Sec. II to introduce our notation, describe the realistic H_{eff} and to outline our approach. The centroid, width, and skewness of the H_{eff} DOS function are the primary inputs for our MM calculations. In Sec. III we describe how the centroid, width, and skewness change as one proceeds from the model Hamiltonian of I to the realistic H_{eff} which we employ. The question of the optimum basis dimensionality is addressed in Sec. IV. MM results for the absolute g.s. energy of ^{16}O and for the Coulomb energies of $A=16$ nuclei indicate that the harmonic oscillator basis employing the first four major shells is optimum. Our main results for relative binding energies as calculated in such a basis are presented in Sec. V. We conclude in Sec. VI with a summary of our findings.

II. CONVENTIONS AND PRELIMINARIES

We generally follow the notations of I for basis states, truncation schemes, and DOS distributions and their characteristics. However, we add a gap operator $\hat{C}$ to the basis Hamiltonian which boosts the energies of selected states. Many-body eigenstates, $|\phi_i\rangle$, of the modified harmonic oscillator (h.o.) Hamiltonian

$$H_0=T+U+\hat{C}\ ; \tag{1}$$
$$T=\sum_{k=1}^{N+Z}\frac{-\hbar^2}{2m}\nabla_k^2,\quad U=\sum_{k=1}^{N+Z}\tfrac{1}{2}m\omega^2|x_k|^2$$

then serve as expansion states for our treatment of a nuclear system with N neutrons and Z protons. We fix $\hbar\omega=14$ MeV which is appropriate to nuclei with $A=N+Z\approx 16$, and we confine our calculations to systems having $14\le A\le 18$. Single-particle (s.p.) eigenstates of H_0 carry the usual labels (n, l, $s=\frac{1}{2}$, j, m_j, $t=\frac{1}{2}$, and t_z) but now have energies

$$\epsilon=\hbar\omega(2n+l+\tfrac{3}{2})+C,\quad 2n+l>N_E$$

(excluded s.p. states),

$$\epsilon=\hbar\omega(2n+l+\tfrac{3}{2}),\quad 2n+l\le N_E$$

(active s.p. states).

Note that the s.p. states have been partitioned into "active" and "excluded" groups according to energy (energy truncation scheme), and that the gap operator $\hat{C}$ of Eq. (1) is defined to boost the energy of each excluded s.p. state by an amount C. The active orbits constitute a "no-core" model space.

For fixed N_E, the finite expansion basis $\{|\phi_i\rangle; i=1,2,\ldots,D\}$ consists of all Slater determinants which can be constructed by distributing the $N+Z$ particles among the active s.p. states. The gap operator $\hat{C}$ has no effect on the H_0 eigenstates which are retained in the expansion basis, and thus has no effect upon the results presented in I. However, due to truncation, $\hat{C}$ does affect our realistic effective nuclear Hamiltonian, H_{eff}, obtained for the no-core model space.

We present calculations only for $N_E=2,3,4,5$, and we denote the associated bases by $E20$, $E40$, $E70$, and $E112$, respectively, in accordance with I. The bulk of the results we report are for the $E40$ basis in which the active s.p. states are confined to the first four major oscillator shells. For $E40$, dimensionalities for nuclei near ^{16}O are $D\sim 10^{16}$.

The nuclear Hamiltonian used in the present study has the form

$$H_{\text{eff}}=T_{\text{rel}}+V_{\text{eff}}+V_{\text{Coul}}\ , \tag{2}$$

where T_{rel} is the relative kinetic energy operator, V_{eff} is an effective N-N interaction obtained from the Reid soft-core interaction,[8] and V_{Coul} is the Coulomb interaction between protons. The methods used to calculate V_{eff} as a function of C and N_E have been presented elsewhere.[6,9] In this work we have improved upon previous calculations of the no-core V_{eff} by including the lowest order folded diagram along with the standard G-matrix term. This additional diagram weakens the C dependence of V_{eff} as may be expected. To gauge the importance of this correction we note that some V_{eff} matrix elements in the $N_E=2$ space changed by as much as 25% at small C values when the folded diagram was included. The corresponding matrix elements changed by only a few percent in the $N_E=5$ space.

We have sought to include the most important contributions to H_{eff} at the two-body interaction level with the hope that MM's would permit us to evaluate physically interesting quantities in sufficiently large model spaces that we could neglect effective three- and higher-body interactions. Recall that without a core there can be no core-polarization—type diagrams. The residual C dependence of our results provides a gauge for the extent to which this level of approximation can be justified. For the basis size used in the bulk of our calculations, we find that the relative binding energies of the nuclei we consider are, indeed, rather C independent over a broad range.

For fixed (N,Z) the full diagonalization of the matrix

$$\{\langle\phi_i|H_{\text{eff}}|\phi_i'\rangle;\ i,i'=1,2,\ldots,D\}$$

would result in D eigenvalues $E_1\le E_2\le\cdots\le E_D$ which define the *calculated* total DOS distribution

$$\rho(E)=\sum_{l=1}^{D}\delta(E-E_l)\ . \tag{3}$$

The exact moments of $\rho(E)$ can be determined without detailed knowledge of the E_l [see Eq. (7) of I] by using the trace reduction techniques of Ginocchio and Ayik.[10,11] To obtain an estimate of the calculated g.s. energy, E_1, one first constructs an approximation $\rho_a(E)$ with the same dimensionality and first few moments as ρ. $\rho_a(E)$ is then integrated from $-\infty$ to an energy E_a where an area of $\frac{1}{2}$ state is first accumulated,[12] and $E_a(N,Z)$ becomes the MM estimate of $E_1(N,Z)$.

For a two-body Hamiltonian such as H_{eff} computation times for the higher moments of $\rho(E)$ grow rapidly with the number of active s.p. states. We have calculated the first two moments for bases through $E112$, and the first three moments for $E20$ and $E40$ bases. This has been done for a variety of C values. As in I we use $\langle E\rangle$, σ, and γ to denote the centroid, width, and skewness of $\rho(E)$, respectively. Again we employ the Gaussian (ρ_{G2}), and

three-moment Weibull distribution (ρ_W) as candidates for continuous ρ_a functions.

The accuracy of the MM in estimating E_1 depends upon how well $\rho_a(E)$ approximates $\rho(E)$ in the region of interest. The use of functional forms based on the Gram-Charlier series was originally motivated by the assumption that $\rho(E)$ would be not too far from Gaussian for large bases. This assumption was found in I to be untrue for the energy-truncated, no-core bases. Furthermore, the Gram-Charlier series with three or more moments can have regions of negative density of states which can lead to ambiguities in predicting the ground state energy. This difficulty led us to investigate the three-moment Weibull distribution in I since it is guaranteed to be positive everywhere. However, the Weibull results tended in I to be comparable with those obtained using the two-moment Gaussian, and it is not clear how to improve the Weibull results in any systematic manner when higher moments are available.

The accumulation of these reasons leads us to introduce here an alternative class of ρ_a candidates. These are adjustable *discrete* DOS distributions constructed by distributing noninteracting nucleons among a collection of s.p. states in all possible ways consistent with the Pauli principle. In each case we begin with a seed spectrum specified by dimensionless input energies

$$\{\epsilon_i \geq 0;\ i=1,2,\ldots,k\}$$

and degeneracies

$$\{d_i;\ i=1,2,\ldots,k\}$$

of s.p. orbitals. This s.p. spectrum is taken to be the same for both protons and neutrons. We then apply a simple three-parameter power transformation

$$\epsilon_i' = b\epsilon_i^p + c,\quad i=1,2,\ldots,k \tag{4}$$

to generate a new set of s.p. energies. For fixed (p,b,c) the associated discrete $\rho_a(E)$ is constructed by enumerating the distinct ways of distributing $N+Z$ noninteracting nucleons among the orbitals $\{\epsilon_i',d_i\}$. The corresponding E_a is then simply the lowest-energy multiparticle state contributing to $\rho_a(E)$. The numerical integration used to determine E_a for each continuous ρ_a is not required for the discrete ρ_a.

The parameters (p,b,c) in Eq. (4) are chosen such that the resulting $\rho_a(E)$ has the first three moments of the $\rho(E)$ we wish to approximate. In addition $\sum_{i=1}^{k} d_i = d$ must equal the number of active single proton (neutron) states in the harmonic oscillator basis. This ensures that ρ_a and ρ have the same total dimensionality as well. Since the moments of $\rho(E)$ vary with the number of nucleons, different (p,b,c) are required for each (N,Z).

A different discrete $\rho_a(E)$ is generated by each choice of input $\{\epsilon_i,d_i\}$. We have chosen three input s.p. spectra with quite different degeneracy structures so that it is easy to observe the sensitivity of the output E_a to variations in the inputs. In each case the scale of the dimensionless E_i has been chosen by fixing $\epsilon_1=0$ and $\epsilon_2=1$. When approximating $\rho(E)$ in an $E40$ basis, the three ordered sets of inputs are

$$\begin{aligned}
\rho_{\rm HO}:&\ \{\epsilon_i\}=\{0,1,2,3\}\ ,\\
&\ \{d_i\}=\{2,6,12,20\}\ ;\\
\rho_{\rm SM}:&\ \{\epsilon_i\}=\{0,1,1.3,1.8,2.1,2.3,2.5,2.8,3.0,3.3\}\ ,\\
&\ \{d_i\}=\{2,4,2,6,2,4,8,4,2,6\}\ ;\\
\rho_{\rm ES}:&\ \{\epsilon_i\}=\{0,1,2,\ldots,19\}\ ,\\
&\ \{d_i\}=\{2,2,2,\ldots,2\}\ .
\end{aligned} \tag{5}$$

The $\{\epsilon_i,d_i\}$ for $\rho_{\rm HO}$ are recognized to be those of a h.o. Hamiltonian. The s.p. energies and degeneracies for $\rho_{\rm SM}$ are typical of a one-body nuclear shell model Hamiltonian. The specific $\{\epsilon_i,d_i\}$ values listed for $\rho_{\rm SM}$ in Eq. (5) are taken from the single-neutron orbitals found by Flocard and Quentin in a density dependent Hartree-Fock (DDHF) calculation of ^{16}O using the Skyrme III interaction.[13] The inputs for $\rho_{\rm ES}$ describe equally spaced s.p. orbitals of degeneracy 2. Because of this diffuse structure, $\rho_{\rm ES}$ is closest in spirit to the continuous ρ_a. The inputs in Eqs. (5) can be truncated or expanded in an obvious manner to form inputs appropriate to expansion bases that are smaller or larger than $E40$.

In practice, the enumeration of the

$$D=\begin{bmatrix} d \\ N \end{bmatrix}\begin{bmatrix} d \\ Z \end{bmatrix}$$

states comprising each discrete ρ_a is not necessary. The skewness of a discrete ρ_a is independent of the values of b and c in Eq. (4) and may be written as a function of p and the $\{\epsilon_i,d_i\}$ by using trace reduction techniques. Thus p is fixed by the known skewness of $\rho(E)$. b and c are then chosen in turn to reproduce the width and centroid of ρ. The s.p. spectra $\{\epsilon_i,d_i\}$ determined by this process are displayed in Fig. 1 for a typical application to $H_{\rm eff}$. Here values of p substantially less than 1 are required to reproduce the large skewness found for the realistic nuclear Hamiltonian ($p=0.66,0.66,0.31$ for $\rho_{\rm HO}$, $\rho_{\rm SM}$, $\rho_{\rm ES}$, respectively, in Fig. 1). This suggests that large rearrangement energies are associated with highly excited states of these nuclei.

III. CHARACTERISTICS OF THE DOS DISTRIBUTION

$H_{\rm eff}$ differs in several important respects from the h.o. Hamiltonian which was treated by MM in I: the removal of the center-of-mass (c.m.) kinetic energy; the inclusion of the Coulomb repulsion between protons; and the presence of a strong (even though renormalized) two-nucleon interaction. We depict the different $\rho(E)$ characteristics for model and realistic Hamiltonians in Fig. 2 for the $E40$ expansion basis. Here H_1 is an energy-shifted version of the h.o. basis Hamiltonian with a potential

$$U'=\sum_{k=1}^{N+Z}\left(\tfrac{1}{2}m\omega^2\,|\,x_k\,|^2-36.625\ \text{MeV}\right).$$

The energy shift is included to facilitate the comparison of model and realistic results in Sec. IV, and it has been chosen such that H_1 has a g.s. energy of -82 MeV for the $N=Z=8$ system. This is the g.s. energy obtained in the exp(s) calculation of ^{16}O using the Reid and Coulomb potentials.[1]

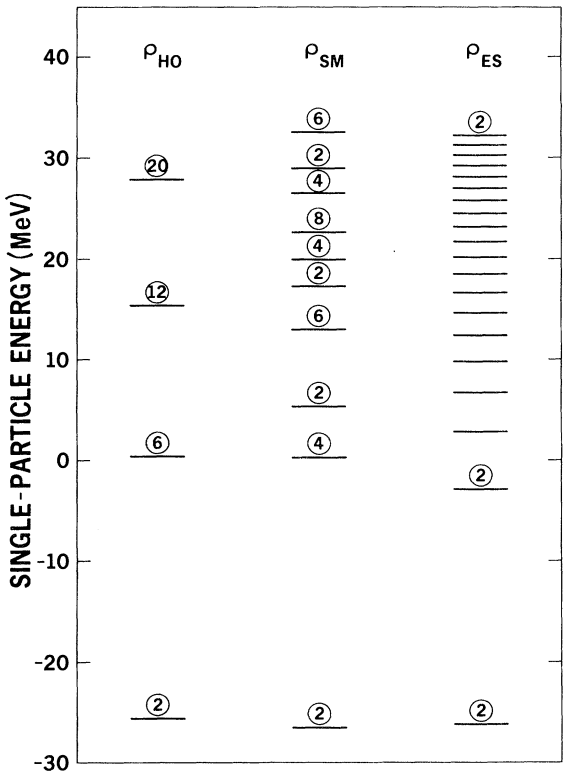

FIG. 1. Adjusted single particle spectra for the discrete distributions ρ_{HO}, ρ_{SM}, and ρ_{ES} in a particular application to ^{16}O. The s.p. spectra are assumed to be identical for neutrons and protons, and the degeneracies of the levels for each type of particle are shown (each *ES* level is twofold degenerate). The three discrete density-of-states distributions have the same dimensionality, centroid, width, and skewness as would be obtained from the diagonalization of H_{eff} (^{16}O) in an $E40$, $C=20$ MeV basis of harmonic oscillator eigenfunctions. To obtain ρ_{HO}, for example, one enumerates the energies of the 5.9×10^{15} ways of distributing 8 neutrons and 8 protons among the 80 single-particle states shown. The ground-state energies of ρ_{HO}, ρ_{SM}, and ρ_{ES} are -98.2, -82.9, and -78.4 MeV, respectively.

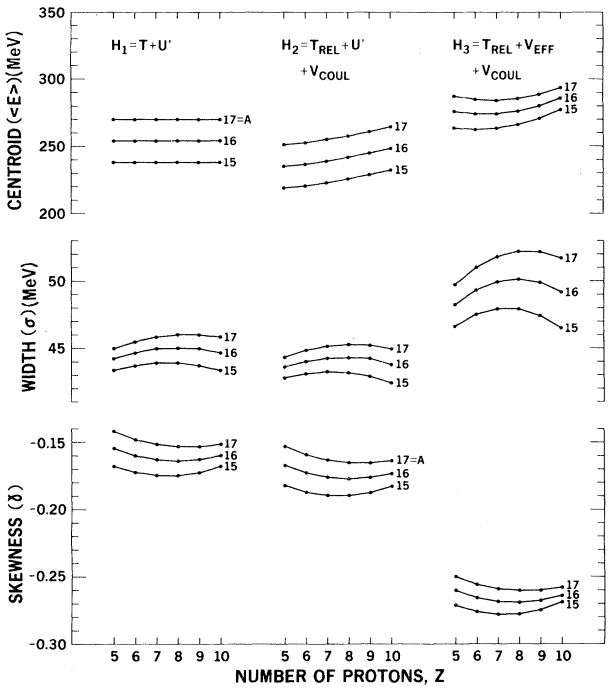

FIG. 2. Characteristics of the DOS distributions $\rho(E)$ for three Hamiltonians as functions of particle numbers A and Z. $\rho(E)$ is the density of calculated eigenvalues which would result from the diagonalization of H_i in an $E40$, $\hbar\omega=14$ MeV, $C=20$ MeV basis of harmonic oscillator eigenfunctions. H_1 is an energy-shifted version of the basis Hamiltonian, and H_3 is the effective Hamiltonian for the finite basis, H_{eff} of Eq. (2).

The progression of panels from left to right in Fig. 2 is intended to indicate the changes which occur as the Hamiltonian becomes more realistic. The removal of the c.m. energy lowers the energy expectation value of each basis state by an amount which generally grows with increasing unperturbed basis energy. For $N=Z=8$

$$\langle \phi_i \mid T-T_{\text{rel}} \mid \phi_i \rangle$$

is about 11 MeV for the lowest unperturbed state, but averages 32 MeV for basis states having all 16 particles in the fourth major shell. The net effect upon $\rho(E)$ of replacing T by T_{rel} in H_1 is to lower $\langle E \rangle$ by 23 MeV, to decrease σ by 1%, and to increase $|\gamma|$ by 9% for ^{16}O, with similar changes for neighboring nuclei. The addition of V_{Coul} produces a similar differential shift which also tends to compress the calculated eigenvalues toward their mean. For $N=Z=8$, $\langle \phi_i \mid V_{\text{Coul}} \mid \phi_i \rangle$ equals 14 MeV for the lowest unperturbed state, while averaging only 10 MeV for basis states constructed from s.p. states in the fourth major shell. The effect of adding V_{Coul} to $T_{\text{rel}}+U'$ in Fig. 2 is to increase $\langle E \rangle$ by 11 MeV and to reduce both σ and $|\gamma|$ by 0.6% for ^{16}O. For fixed A, and increasing Z, the Coulomb interaction produces a simple rise of the H_2 centroids.

Not surprisingly, the effect of replacing U' by V_{eff} is seen in Fig. 2 to be considerably more dramatic than the combined effects of c.m. removal and Coulomb addition. The renormalized two-nucleon interaction produces a noticeable increase in width and a particularly large increase in the degree of skewness of $\rho(E)$. For H_1, as for the model problem in I, the $N=Z=8$ skewnesses are -0.070 and -0.164 for the $E20$ and $E40$ bases, respectively, and the skewness approaches -0.215 as the basis size expands ($N_E\rightarrow\infty$). By contrast the H_{eff} ($C=20$ MeV) skewnesses are -0.258 and -0.269 for $E20$ and $E40$, respectively.

The large skewness observed for the realistic Hamiltonian argues against DOS approximations, such as ρ_{Gm}, which are based on a Gaussian form. This is one motivation for considering alternate approximations, such as the adjustable discrete distributions introduced in Sec. II. However, the skewness values obtained in the $E20$ realistic calculations are too large to permit the use of the simple discrete approximations we chose. That is, for $E20$ no

value of p can be found in Eq. (4) such that our discrete ρ_a's possess the H_{eff} skewness. As evidenced by Fig. 1, no similar problem exists for the larger basis spaces where the input s.p. seed spectra are richer.

IV. OPTIMUM BASIS SIZE

As the h.o. expansion basis is enlarged, the approximations used in the construction of H_{eff} are less severe and the lower eigenvalues of H_{eff} should approach those of the full Hamiltonian H ($H=T_{\text{rel}}+V+V_{\text{Coul}}$, V=Reid potential). In particular, as N_E increases, the g.s. eigenvalue of H_{eff} (^{16}O) is expected to converge to some value near the exp(s) result of -82 MeV for all values of C and $\hbar\omega$. However, as the basis is enlarged the error in the MM estimate of the H_{eff} g.s. energy should generally grow if a fixed number of moments are employed. One therefore expects that there will be an optimum basis size where the MM treatment of H_{eff} with a few moments yields the most accurate estimate of the H g.s. energy. The optimal basis size can be estimated by considering the dimensionality dependence of the MM results for the ^{16}O g.s. energy and for Coulomb energies.

A. Calculated g.s. energy of ^{16}O

The MM estimate of the H_{eff} ^{16}O g.s. energy is displayed in Fig. 3 for various choices of C, N_E, and the form of the DOS approximation $\rho_a(E)$. As the expansion basis is enlarged, the C dependence of the H_{eff} g.s. energy is expected to moderate. This feature is observed in Fig. 3 for the energy estimate from each of the three continuous distributions. As seen in I, the absolute errors in the MM estimates are expected to grow with increasing basis dimensionality. This trend is also evidenced in Fig. 3 by the divergence of the various MM estimates from one another as we proceed from $E20$ to $E40$.

MM estimates of the g.s. energy for the shifted h.o. Hamiltonian, H_1 of Fig. 2, have been included in Fig. 3 for comparison. Since the exact binding energy of H_1 is known (5.125 MeV per particle for $N=Z=8$), the errors in the MM estimates of the H_1 g.s. are manifest in Fig. 3. For $E40$, ρ_{ES} and ρ_{SM} lead to too little binding for H_1, ρ_{HO} reproduces the exact result, and the three continuous DOS approximations lead to overbinding. Similar orderings and spreads of the MM estimates are observed for H_1 and H_{eff}. Thus, the dependence of the H_{eff} results on the choice of MM ingredients is so systematic as to be understandable from the soluble model applications. If we make a simple "correction" of each $E40$ H_{eff} estimate by subtracting the known error in the corresponding H_1 MM calculation, the results lie in a band approximately bounded by the present ρ_{HO} and ρ_{W} curves in Fig. 3.

As we proceed from $E20$ to $E40$ in Fig. 3, the MM estimates are seen to generally rise toward the exp(s) value. However, this trend appears to reverse as we further enlarge the basis. The centroid and width of $\rho(E)$ have been calculated for the next two larger bases, $E70$ and $E112$. If we assume that the H_{eff} skewness increases slowly with D as the model problem of I, e.g., that $\gamma\approx-0.28\pm0.02$ for ^{16}O in an $E70$ $C=20$ basis, we can estimate the three-moment E_a values for the larger spaces. The effect of proceeding from $E40$ to $E70$ is then generally a small clockwise rotation and downward shift of the $E40$ curves

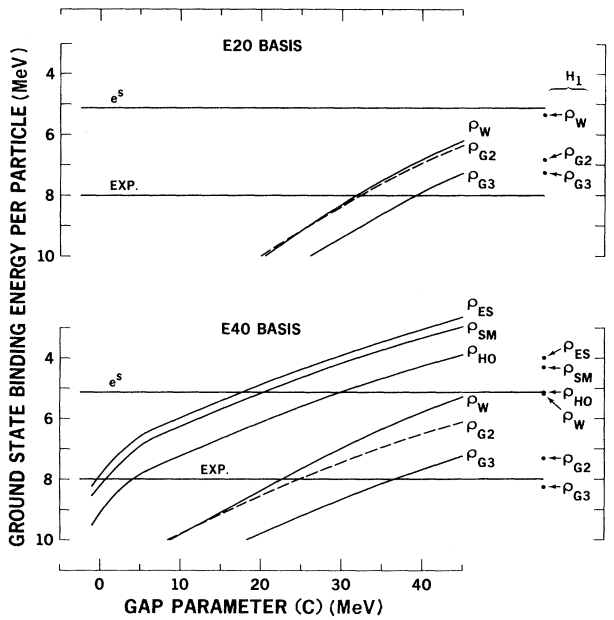

FIG. 3. Ground state binding energy per particle of H_{eff} (^{16}O) as a function of the basis gap parameter for the $E20$ and $E40$ bases. The moment method estimate ($-E_a/16$) is displayed for six choices of the DOS approximation $\rho_a(E)$. Each distribution, with the exception of the Gaussian (ρ_{G2}), has the first three moments of the DOS which would result from the diagonalization of H_{eff} in the basis. The experimental binding energy of ^{16}O and the result of an exp(s) calculation (Ref. 1) are also shown. Points in the far right-hand column are g.s. estimates resulting from the application of MM to the shifted harmonic oscillator Hamiltonian H_1 (^{16}O) of Fig. 2. The exact H_1 g.s. energy coincides with the exp(s) value.

in Fig. 3. For example, the $E70$ ρ_{SM} estimate ranges from

$$9.3\gtrsim -E_{\text{SM}}/16\ \text{MeV}\gtrsim 5.3$$

on $-1\leq C/\text{MeV}\leq 45$, while the $E70$ Gaussian estimate ranges over $11.3\gtrsim -E_{G2}/16$ MeV $\gtrsim 7.6$. This downward shifting of the MM estimates away from the exp(s) value accelerates for the $E112$ basis. Beyond $E40$, the absolute error in the MM technique is evidently growing faster than the reduction in error produced by using H_{eff} in a larger model space.

B. $A=16$ Coulomb energies

Calculations of Coulomb energies provide evidence that errors in *relative* energies are also smallest in the $E40$ basis. For fixed N and Z we define the Coulomb energy $\Delta E_c(N,Z)$, as the difference in the g.s. energies of H_{eff} and H_{eff}-V_{Coul}. An estimate of ΔE_c is obtained by applying MM to each of these two Hamiltonians in turn. Results for $A=16$ nuclei are displayed in Fig. 4 for an $E40$ basis. The expected linear dependence of ΔE_c on Z^2 is observed. In fact the $E40$ MM curves for the various choices of ρ_a are seen to bracket the semiempirical result of Myers and Swiatecki[14]:

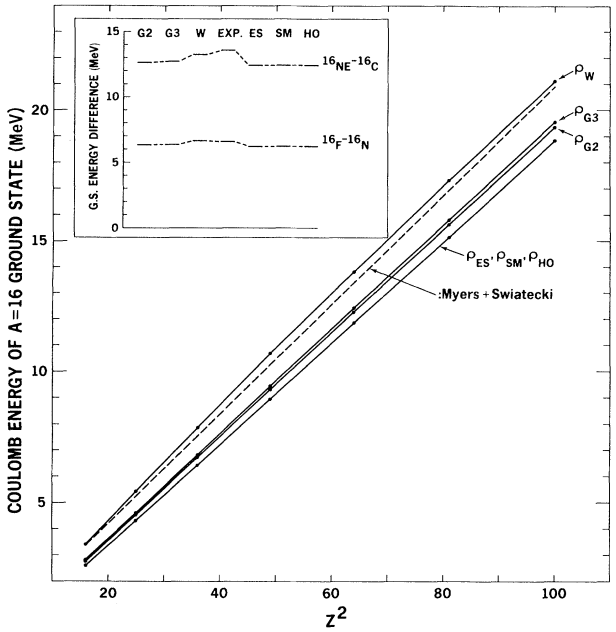

FIG. 4. Moment method estimates of the H_{eff} Coulomb energies of $A=16$, $4\leq Z\leq 10$ systems. Results obtained using a $C=20$ MeV, $E40$ expansion basis are shown for each of the six DOS approximations discussed in the text (solid curves). The three discrete approximations lead to nearly coincident results. The semiempirical result of Myers and Swiatecki (Ref. 14), Eq. (6), which summarizes the experimental data is shown for comparison. The inset displays the MM estimated g.s. difference $E_a(N,Z)-E_a(Z,N)$ for two pairs of mirror nuclei when the Coulomb potential is retained in H_{eff}. Again the basis is $E40$, $C=20$ MeV. The experimental energy differences are taken from Ref. 15.

$$\Delta E_c=\frac{0.717Z^2}{A^{1/3}}\left[1-\frac{1.69}{A^{2/3}}\right]\text{ MeV}\ . \tag{6}$$

Calculated Coulomb energies exhibit little dependence on the basis gap parameter, and the bracketing of the semiempirical result occurs for all $-1\leq C/\text{MeV}\leq 45$ in the $E40$ basis. Differences in the g.s. energies of mirror nuclei, which are due solely to the Coulomb term in H_{eff}, are similarly well reproduced by $E40$ MM calculations, as illustrated by the inset in Fig. 4.

As the expansion basis is enlarged, we expect that ΔE_C resulting from the actual diagonalizations of H_{eff} and H_{eff}-V_{Coul} would stabilize, presumably near the value given by Eq. (6). However, we find that the MM estimates of ΔE_c show clear evidence of diverging from the semiempirical result as the basis size increases beyond $E40$. As the basis dimensionality is increased, the MM estimates of ΔE_c drop steadily, and the semiempirical result is not bracketed beyond $E40$. We interpret this as further indication that errors inherent in the moment method outstrip the reduction in H_{eff} renormalization errors for bases beyond $E40$ when only three moments are used to fix $\rho_a(E)$.

In summary, errors in total and relative binding energies for the full Hamiltonian are evidently smallest when MM's are applied to H_{eff} in the $E40$ basis. We consequently confine our calculations to $E40$ for the remainder of this work.

V. CALCULATED RELATIVE ENERGIES FOR NUCLEI NEAR ^{16}O

Errors in MM estimates of relative binding energies were generally found in I to be substantially smaller than errors in total binding energies. We now apply MM's in an $E40$ basis to evaluate the relative binding energies of $14\leq A\leq 18$ nuclei using the realistic no-core effective Hamiltonian. With reasonable choices of MM ingredients, we obtain relative binding energies which are in good agreement with experiment and only weakly dependent on C.

A. Gap parameter dependence

The residual C dependence of the total binding energy is the price we must pay for working in a limited basis. For $E40$ the triplet $(\langle E\rangle/\text{MeV}, \sigma/\text{MeV}, \gamma)$ of $\rho(E)$ characteristics for H_{eff} is (246,54,−0.30), (276,50,−0.27), and (304,47,−0.23) for $C=-1$, 20, and 55 MeV, respectively. These are examples of the moment variations which result in the C dependence of the total ^{16}O binding energy estimates depicted in the lower portion of Fig. 3.

Calculated *relative* g.s. energies, particularly those within a given A chain, exhibit much less C dependence than absolute energies. For a given choice of the ρ_a form, the g.s. energy difference between a pair of nearby nuclei is generally observed to fall monotonically as C is increased. That is, as the calculated absolute binding energy of ^{16}O falls, energy separations fall as well.

To quantitatively describe the C dependence of relative g.s. energies it is helpful to introduce

$$\Delta_1=E_a(N=6,Z=8)-E_a(10,8)$$

and

$$\Delta_2=E_a(11,5)-E_a(8,8)\ .$$

These are measures of the energy separation between A chains, and the energy variation within A chains, respectively. The experimental counterparts of Δ_1 and Δ_2 are each near 40 MeV. The following rule of thumb summarizes our MM calculations: For a given ρ_a in an $E40$ basis, a 6 MeV increase in C results in a 10 MeV decrease in the calculated ^{16}O binding energy, a 4 MeV decrease in Δ_1, and a 1 MeV decrease in Δ_2. Energy differences within an A chain are thus quite stable to changes in C, while the energy separation between A chains is more strongly tied to the calculated ^{16}O energy.

B. Comparison with experiment

Calculated g.s. energies, relative to ^{16}O, are displayed in Fig. 5 for each of our six choices of the ρ_a form. Different gap parameters have been used for the continuous and discrete ρ_a so that the predicted ^{16}O g.s. energy is roughly the same for each distribution, i.e., slightly below the experimental value (see Fig. 3). This facilitates the

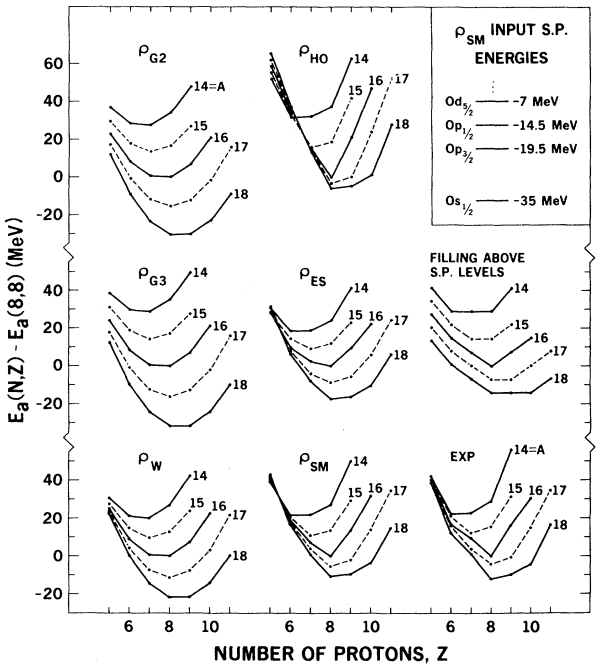

FIG. 5. Calculated g.s energies for $14 \leq A \leq 18$ nuclei relative to the calculated ^{16}O energy. In the left and central columns, MM estimates of $H_{eff}(N,Z)$ relative energies are shown for six choices of the DOS function $\rho_a(E)$. In each case an $E40$ expansion basis was used, with $C=20$ MeV for $\{\rho_{G2},\rho_{G3},\rho_W\}$, and $C=-1$ MeV for $\{\rho_{HO},\rho_{ES},\rho_{SM}\}$. The third column displays the Flocard-Quentin (Ref. 13) single-neutron orbits which are used in the seed $\{\epsilon_i,d_i\}$ for ρ_{SM}. The g.s. energy spectrum which results from filling these fixed orbits with neutrons and protons, consistent with the Pauli principle, is also shown. The experimental energy differences are those of Ref. 15.

comparison of A-chain separations which are generally found to be proportional to the ^{16}O energy. The appearances of the predicted g.s. energy patterns at other values of C may be inferred from Fig. 5 and the stated rule of thumb for the Δ_i.

When compared with experiment, the continuous ρ_a results in Fig. 5 exhibit the same strengths and deficiencies that were observed in I. Average A-chain separations are reasonably well reproduced, particularly for ρ_W, but too small a variation within each A chain is found. Closed shell phenomena, such as the energy gap between ^{16}O and its immediate $A=16$ neighbors, are again not reproduced by the MM calculations employing continuous ρ_a. When the Gram-Charlier series is used to approximate the H_{eff} DOS, there is no evident improvement in the results when third-moment information is added. However, a noticeable movement toward experiment occurs when the Gaussian is replaced by the three-moment Weibull distribution.

As a group, the three discrete distributions do much better in predicting relative energies within A chains. ρ_{ES}, which is closest in spirit to continuous ρ_a, leads to relative energy estimates similar to those of the Weibull distribution. ρ_{SM}, whose input s.p. spectrum is between the ρ_{ES} and ρ_{HO} extremes, does very well in reproducing the overall appearance of the experimental relative energy pattern.

It is enlightening to ask to what extent are the ρ_{SM} MM results of Fig. 5 *guaranteed* to be good simply by the choice of a realistic input s.p. spectrum? To answer this question, we include in Fig. 5 the binding energy pattern obtained by simply placing particles into the lowest available states of the DDHF single-particle potentials from which the $\{\epsilon_i,d_i\}$ for ρ_{SM} are taken. This corresponds to using the power transformation formula with parameters $(p,b,c,)=(1,\ 15.5\ \text{MeV},\ -35\ \text{MeV})$ for all (N,Z), or, equivalently, to neglecting all information from the calculated moments of H_{eff}. Clearly the moment results are crucial for obtaining the good agreement with experiment shown for ρ_{SM} in Fig. 5.

The choice of the seed s.p. inputs for the adjustable discrete distribution, $\{\epsilon_i,d_i\}$, is highly arbitrary, although the most reasonable of our three choices (ρ_{SM}) is seen to lead to the best agreement with experiment. Rather than freely choosing the $\{\epsilon_i,d_i\}$, one can use an input set generated by the Hamiltonian being treated. As an example of such a procedure, we have performed a spherical Hartree-Fock (SHF) calculation on H_{eff} $(N=Z=8)$ in the $E40$ basis and used the resulting single-neutron orbits to fix the $\{\epsilon_i,d_i\}$. This was done for each value of the gap parameter. With the $\{\epsilon_i,d_i\}$ thus fixed by the ^{16}O SHF calculation, the power transformation method was used for each (N,Z) to match the associated discrete distributions (ρ_{SHF}) to the first three moments of H_{eff}. The lowest eigenvalue of $\rho_{SHF}(E)$ was then the MM estimate of the H_{eff} g.s. energy.

In the ρ_{SHF} calculations, the C dependence of absolute and relative energies was again found to follow the rule of thumb started earlier; at the $E40$ level, calculated energy differences within A chains were the least dependent on the choice of C, and hence the most meaningful. These energy differences are displayed in Fig. 6 for the limits of the range $(-1 \leq C/\text{MeV} \leq 55)$ within which we have calculated H_{eff}. Clearly, the dependence of MM relative binding energies on the value of C is rather weak and the overall agreement with experiment is quite good.

The residual discrepancies in Fig. 6 between the ρ_{SHF} results and experiment appear to be due to too little spin-orbit splitting, consistent with the long-standing problem with realistic interactions in nuclear theory. Our SHF spin orbit splittings are similar to the coupled-cluster results of Ref. 2. ρ_{SM} results, which have been included in Fig. 6, are seen to be consistently closer to experiment. The s.p. seed spectrum for ρ_{SM}, which is taken from phenomenological DDHF results using the Skyrme III interaction,[13] exhibits considerably more spin-orbit splitting than is found in the SHF H_{eff} calculation. The input energy spacings of the lowest four s.p. orbits $(0s_{1/2},0p_{3/2},0p_{1/2},0d_{5/2})$ have the greatest influence on the MM results, since these orbits are partially or fully filled for $14 \leq A \leq 18$ nuclei. For ρ_{SM} the $0p_{1/2}$-$0d_{5/2}$ energy gap is about 35% smaller than that of ρ_{SHF}, due to the larger $0d_{5/2}$-$0d_{3/2}$ splitting in the former. By suitably increasing the $0d_{5/2}$-$0d_{3/2}$ splitting in the ρ_{SHF} input list, $\{\epsilon_i,d_i\}$, the ρ_{SHF} results in Fig. 6 can be made nearly identical with those of ρ_{SM}. This could be an indication that

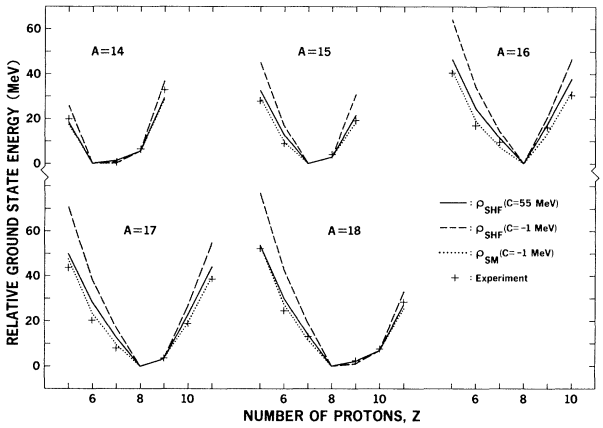

FIG. 6. Ground state energies within A chains, relative to the lowest-energy member of the chain. The H_{eff} MM estimate of $E_a(N,Z)-E_a(N_0,Z_0)$ is displayed where $(N_0,Z_0)=(8,6)$, (8,7), (8,8), (9,8), and (10,8) for $A=14$, 15, 16, 17, and 18, respectively. The corresponding experimental energy differences are taken from Ref. 15. MM results in an $E40$ basis are shown for two choices of the approximate DOS distribution. For ρ_{SHF} the seed inputs, $\{\epsilon_i,d_i\}$ in Eq. (4), are taken from a spherical Hartree-Fock calculation of H_{eff} ($N=Z=8$). The seed inputs for ρ_{SM} are from a density dependent Hartree-Fock calculation (Ref. 13). The degree of C dependence is similar for the ρ_{SHF} and ρ_{SM} results.

difficulties with theoretical binding energies of nuclei are closely tied to the problem of theoretical spin-orbit splittings.

VI. SUMMARY

We have used moment methods with a realistic H_{eff} to obtain binding energies of nuclei with $14\leq A\leq 18$. In addition to the continuous density-of-states functions employed in I, we have introduced a class of adjustable discrete DOS functions. Each discrete function is generated from a list $\{\epsilon_i,d_i\}$ of input s.p. energies and degeneracies. The ϵ_i are modified by a simple power transformation to yield a many-body spectrum in agreement with the calculated first three moments of H_{eff}. The choice of the input set $\{\epsilon_i,d_i\}$ thus replaces the choice of functional form one makes when employing a continuous DOS distribution. We have used three diverse choices of $\{\epsilon_i,d_i\}$ in the preliminary calculations to illustrate the degree to which output binding energies are dependent on the input list.

While the choice of a power law transformation, such as Eq. (4), is convenient for matching moments of the realistic spectra to moments of the discrete DOS functions, it also provides a simple picture of the behavior of the system at high excitation energies. That is, when we choose a "realistic" input s.p. spectrum such as a Hartree-Fock or phenomenological shell model spectrum, the moments require a substantial compression of the high-lying s.p. spectra. This indicates large rearrangement energies are associated with highly excited states of these nuclei. On this basis we may also conclude that the adjustable discrete DOS method proposed here should be helpful in relating knowledge of nuclear level densities to realistic effective Hamiltonians.

The approximations employed fall into two major categories: the neglect of effective many-body forces in obtaining H_{eff} for no-core model spaces, and the approximation of obtaining the ground state energy of H_{eff} from only its few lowest moments. As the model space size is increased, the error in the g.s. energy induced by neglecting many-body forces should fall, while the error in the MM estimation process with a fixed number of moments is expected to grow.[7] By a comparison with the exp(s) results[1] for ^{16}O we find an optimum balance of diminishing errors in H_{eff} and increasing errors in MM is obtained with an $E40$ basis. (Such a basis contains 5.9×10^{15} Slater determinants for ^{16}O.) The choice of $E40$ as the optimal basis size for the $A=16$ region when three moments of H_{eff} are used is supported by Coulomb energy calculations.

The importance of neglected effective many-body forces is gauged by the residual dependence of binding energies on the gap parameter C. For the $E40$ basis, the binding energy per particle for ^{16}O changed by approximately 1 MeV for each change of 10 MeV in C (Fig. 3). However, calculated relative binding energies within an A chain were found to be nearly independent of C (Fig. 6).

Relative binding energies calculated using continuous DOS functions displayed the same successes and shortcomings that were observed in the model calculations of I. In particular, the continuous functions led to too small a variation of predicted binding energies within each A chain. Discrete DOS functions generated using sensible choices of $\{\epsilon_i,d_i\}$ were much more successful in reproducing experimental energy separations with A chains. An input list based on the HF spectrum from H_{eff} was found to be quite adequate, but a DDHF s.p. spectrum led to improved agreement with experimental relative binding energies due to a more accurate spin-orbit splitting.

The main results of this work are presented in Fig. 6 and show that, where the methods employed are most stable, we obtain good agreement between theoretical and experimental relative binding energies within each A chain. We view with satisfaction the accurate prediction of the most stable isobar in all cases.

The current effort does not begin to address the potential advantages of partitioning model spaces according to some symmetry scheme.[16] However, future progress in applications of realistic effective Hamiltonians in large model spaces will depend upon successfully implementing methods of partitioning the space.

ACKNOWLEDGMENTS

We wish to acknowledge many useful discussions with B. J. Dalton and R. H. Belehrad. This work was supported in part by the U.S. Department of Energy Contracts Nos. W-7405-ENG-82 and DE-AC02-82ER40068, Division of High Energy and Nuclear Physics.

[1]H. Kummel, K. H. Luhrmann, and J. G. Zabolitzky, Phys. Rep. 36C, 1 (1978), and references therein.
[2]J. G. Zabolitzky and W. Ey, Nucl. Phys. A328, 507 (1979).
[3]K. Emrich and J. G. Zabolitzky, Nucl. Phys. A351, 439 (1981).
[4]B. J. Dalton, J. P. Vary, and W. J. Baldridge, Phys. Rev. Lett. 38, 1348 (1977).
[5]J. P. Vary, R. Belehrad, and B. J. Dalton, Nucl. Phys. A328, 526 (1979).
[6]J. P. Vary, in *Theory and Application of Moment Methods in Many-Fermion Systems,* edited by B. J. Dalton, S. M. Grimes, J. P. Vary, and S. A. Williams (Plenum, New York, 1980).
[7]F. J. Margetan, A. Klar, and J. P. Vary, Phys. Rev. C 27, 852 (1983).
[8]R. V. Reid, Ann. Phys. (N.Y.) 50, 411 (1968).
[9]J. P. Vary and S. N. Yang, Phys. Rev. C 15, 1545 (1977).
[10]S. Ayik and J. N. Ginocchio, Nucl. Phys. A221, 285 (1974).
[11]B. D. Chang and S. S. M. Wong, Nucl. Phys. A294, 19 (1978).
[12]We adopt the point of view that the degeneracy of the lowest H_{eff} eigenvalue is not known *a priori*, and we consequently use $q=1$ in Eq. (13) of Ref. 7 throughout the present work when continuous DOS functions are employed.
[13]H. Flocard and P. Quentin, contained in Ph.D. dissertation of H. Flocard, Centre D'Orsay Université Paris-Sud, 1975 (unpublished).
[14]W. D. Myers and W. J. Swiatecki, Nucl. Phys. 81, 1 (1966).
[15]A. H. Wapstra and K. Bos, At. Data Nucl. Data Tables 19, 175 (1977).
[16]See, for example, J. B. French, in *Theory and Applications of Moment Methods in Many-Fermion Systems,* Ref. 6, p. 1.